Optical Materials 33 (2011) 1591–1594

Contents lists available at ScienceDirect

Optical Materials

journal homepage: www.elsevier.com/locate/optmat

Dynamical processes of energy transfer in red emitting phosphor $CaMoO_4:Sm^{3+}$, Eu^{3+}

Ye Jin [a,b], Zhendong Hao [a], Xia Zhang [a], Yongshi Luo [a], Xiaojun Wang [a,c,*], Jiahua Zhang [a,*]

[a] Key Laboratory of Excited State Processes, Changchun Institute of Optics, Fine Mechanics and Physics, Chinese Academy of Sciences, 3888 Eastern South Lake Road, Changchun 130033, China
[b] Department of Applied Physics, School of Optoelectronic Information, Chongqing University of Technology, 69 Hongguang Street, Chongqing 400054, China
[c] Department of Physics, Georgia Southern University, Statesboro, GA 30460, USA

ARTICLE INFO

Article history:
Received 10 December 2010
Received in revised form 8 April 2011
Accepted 9 April 2011
Available online 10 May 2011

Keywords:
Dynamical process
Energy transfer
Red phosphor
$CaMoO_4:Sm^{3+}$, Eu^{3+}

ABSTRACT

Upon $^4K_{11/2}$ excitation of Sm^{3+} at 405 nm, the performance of energy transfer from Sm^{3+} to Eu^{3+} in the red emitting phosphor $CaMoO_4:Eu^{3+}$, Sm^{3+} significantly extends its excitation region for better matching the near-UV LED. Photoluminescence spectra indicate that the energy transfer pathway concerns the relaxation from $^4K_{11/2}$ to $^4G_{5/2}$ of Sm^{3+} and subsequent transfer to $^5D_0$ of Eu^{3+} rather than $^5D_1$ of Eu^{3+}. The fluorescent decay pattern of Sm^{3+} $^4G_{5/2}$ level in $CaMoO_4$:0.5% Sm^{3+}, 2% Eu^{3+} is studied at 77 K based on the Inokuti–Hirayama formula, revealing an electronic dipole–dipole interaction between Sm^{3+} and Eu^{3+}. The coefficient for the energy transfer is obtained to be 8.5×10^{-40} s^{-1} cm^6. The fluorescence rise and decay pattern of Eu^{3+} $^5D_0$ level as Sm^{3+} is only excited at 77 K is well described by the dynamical processes of the energy transfer.

1. Introduction

Since the great realization of GaN based blue and/or near-ultraviolet (NUV) light-emitting diode (LED) [1], solid-state lighting based on phosphor converted (pc) white LEDs has attracted much interests because of its great advantages over the conventional incandescent and fluorescent lamps [2–5] in power efficiency, reliability, lifetime and environmental protection [6]. The general strategy of producing white light is to combine a blue LED with a yellow emitting phosphor (YAG:Ce^{3+}). This combination leads to low color rendering index (CRI) because of deficient red component in the yellow phosphor. The combination of a NUV LED with RGB-color phosphors is another alternative, which may provide a high CRI [7] if red emitting phosphors, which are scarce at present, are obtained. Eu^{3+} doped $CaMoO_4$ has been investigated as a potential red emitting phosphor for NUV LED based pc-white LEDs because it exhibits more stable physical and chemical properties than the well-known red phosphor, $Y_2O_2S:Eu^{3+}$ [8]. The red emission is originated from $^5D_0 \rightarrow {}^7F_2$ transition of Eu^{3+} and the NUV excitation performs at around 395 nm through $^7F_0 \rightarrow {}^5L_6$ absorption of Eu^{3+}. Some investigations on enhancing the luminescence intensity of $CaMoO_4:Eu^{3+}$ were reported by introducing Li^+, Na^+, K^+ and Bi^{3+} ions into the phosphor [9–11]. Sm^{3+} was also introduced in $CaMoO_4:Eu^{3+}$, Zhuang et al. compared the luminescence of $CaMoO_4:Eu^{3+}$ with $CaMoO_4:Eu^{3+}$, Sm^{3+} [12]. In our previous work [13], we reported that codoping Sm^{3+} into $CaMoO_4:Eu^{3+}$ can generate additional NUV excitation line at 405 nm, originating from $^6H_{5/2} \rightarrow {}^4K_{11/2}$ absorption of Sm^{3+}. This behavior is proved to be the result of energy transfer from the $^4K_{11/2}$ level of Sm^{3+} to the $^5D_0$ level of Eu^{3+}. The significance of energy transfer is to extend the excitation lines for effectively covering the NUV LED source in the spectral range of 390–410 nm so as to take advantage of whole spectral components of the LED excitation source. The energy transfer from Sm^{3+} to Eu^{3+} has been also investigated in other red emitting phosphors $Na_{0.5}Sm_{0.1}Eu_{0.4}WO_4$ [14], $NaEu(MoO_4)_2$ [15] and other molybdate [16]. However, the physical processes and related parameters in the energy transfer in Sm^{3+} and Eu^{3+} codoped system have not been reported yet.

In this paper, we demonstrate, to our knowledge for the first time, the pathway, interaction mechanism and dynamical processes of energy transfer between Sm^{3+} and Eu^{3+} in $CaMoO_4$ basing on spectroscopic data and the analysis of rise and decay patterns of fluorescence of Sm^{3+} and Eu^{3+} by using Inokuti–Hirayama formula.

2. Experimental

$CaMoO_4:Sm^{3+}/Eu^{3+}$ materials were obtained by solid state reaction in the air as we reported previously [11]. Photoluminescence (PL) and photoluminescence excitation (PLE) spectra were

* Corresponding authors. Address: Key Laboratory of Excited State Processes, Changchun Institute of Optics, Fine Mechanics and Physics, Chinese Academy of Sciences, 3888 Eastern South Lake Road, Changchun 130033, China.
E-mail address: zhangjh@ciomp.ac.cn (J. Zhang, X. Wang).

0925-3467/$ - see front matter © 2011 Elsevier B.V. All rights reserved.
doi:10.1016/j.optmat.2011.04.009

recorded at room temperature using a Hitachi F-4500 spectrophotometer. In luminescent decay curve measurements, 563.32 nm light pulse from an optical parametric oscillator (OPO) was used as excitation source, and the signals were recorded by a Tektronix digital oscilloscope model (Tektronix, TDS 3052, 500 MHz, and 5 Gs/s) with the sample was situated in liquid nitrogen.

3. Results and discussion

The powder X-ray diffraction pattern of $CaMoO_4$:20% Eu^{3+}, 0.5% Sm^{3+} is shown in Fig. 1a. All peaks for the as-prepared sample match well with the standard pattern of a pure $CaMoO_4$ tetragonal structure (JCPDS No. 85-0585). No peaks due to any other phases are detected, indicating the dopant ions do not change the crystal structure of the hosts.

Fig. 1b shows the PLE spectra by monitoring the $^5D_0 \rightarrow {}^7F_2$ emission of Eu^{3+} at 612 nm in Eu^{3+} singly doped and Eu^{3+} and Sm^{3+} doubly doped $CaMoO_4$. Both of the samples show a broad PLE band ranging from 200 nm to 325 nm, which is assigned to the combination of the charge transfer transition of Eu^{3+}–O^{2-} and MoO_4^{2-} group [9]. The sharp PLE line located at around 395 nm is ascribed to the $^7F_0 \rightarrow {}^5L_6$ transitions of Eu^{3+}. The other PLE line at 405 nm, which appears only in the samples containing Sm^{3+}, is ascribed to the $^6H_{5/2} \rightarrow {}^4K_{11/2}$ transition of Sm^{3+}, indicating the performance of energy transfer from Sm^{3+} to Eu^{3+}.

The diffused reflectance spectra of $CaMoO_4$:Eu^{3+} and $CaMoO_4$:Eu^{3+}, Sm^{3+} were measured, as shown in Fig. 2. An absorption edge at 300 nm owing to MoO^{2-} is clearly presented in both the samples and the absorption peaks of intra-4f transitions of Eu^{3+} at 395 and 465 nm, Sm^{3+} at 405 nm are presented. It can be found that the absorption of Eu^{3+} ions enhances with the introduction of Sm^{3+}.

The PL spectra of Sm^{3+} singly doped $CaMoO_4$ under excitation at 405 nm exhibit three characteristic transitions of Sm^{3+}:$^4G_{5/2} \rightarrow {}^6H_{5/2}$ (561 nm), $^4G_{5/2} \rightarrow {}^6H_{7/2}$ (596 nm, 604 nm) and $^4G_{5/2} \rightarrow {}^6H_{9/2}$ (642 nm), as shown in Fig. 3A(a). The PL spectra of Eu^{3+} singly doped $CaMoO_4$ under excitation at 395 nm, consists of series characteristic lines of Eu^{3+} originating from the transitions of $^5D_1 \rightarrow {}^7F_1$ at 534 nm, $^5D_0 \rightarrow {}^7F_1$ at 590 nm and $^5D_0 \rightarrow {}^7F_2$ at 612 nm as shown in Fig. 3A(b). In Eu^{3+} and Sm^{3+} doubly doped $CaMoO_4$, the PL spectra under 395 nm excitation (Fig. 3A(c)) is the same as that of Eu^{3+} singly doped samples, indicating that Sm^{3+} cannot be excited by 395 nm and no pronounced energy transfer from Eu^{3+} to Sm^{3+}. When the doubly doped sample is excited at 270 nm, the characteristic emissions of both Eu^{3+} and Sm^{3+} can be observed, as shown in Fig. 3A(d), indicating the charge transfer state of Eu^{3+}–O^{2-} and MoO_4^{2-} group can transfer energy to both of Eu^{3+} and Sm^{3+}. When

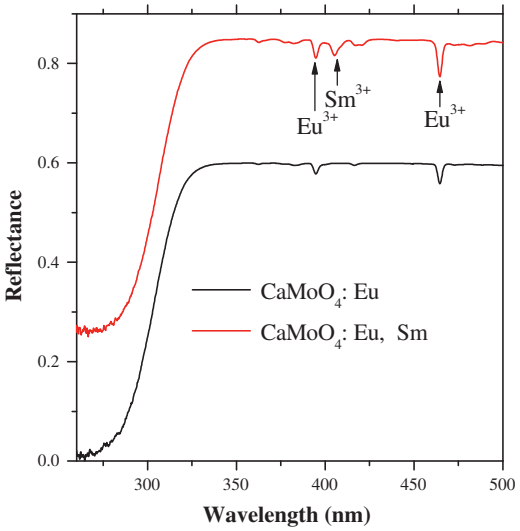

Fig. 2. Diffuse reflection spectra of $CaMoO_4$:Eu^{3+} and $CaMoO_4$:Eu^{3+}, Sm^{3+}.

the doubly doped sample is excited at 405 nm responsible for the $^6H_{5/2} \rightarrow {}^4K_{11/2}$ transition of Sm^{3+}, besides the fluorescence of Sm^{3+}, the fluorescence from $^5D_0 \rightarrow {}^7F_1$ and $^5D_0 \rightarrow {}^7F_2$ transitions of Eu^{3+} is also observed, as shown in Fig. 3A(e). This is the indication of energy transfer from Sm^{3+} to Eu^{3+}. A notable behavior presented in Fig. 3A(e) is that the $^5D_1 \rightarrow {}^7F_1$ emission of Eu^{3+} is not detected at 534 nm. As a result, the energy transfer pathway is proposed as illustrated schematically in Fig. 3B. As the $^4K_{11/2}$ level of Sm^{3+} is excited, it completely relaxes down to the $^4G_{5/2}$ state without energy transfer to Eu^{3+}. Subsequently, the $^4G_{5/2}$ state either returns to the ground states ($^6H_{9/2}$, $^6H_{7/2}$ and $^6H_{5/2}$) to emit or transfers its energy to the $^5D_0$ level not the $^5D_1$ level of Eu^{3+} to produce the $^5D_0 \rightarrow {}^7F_1$ and $^5D_0 \rightarrow {}^7F_2$ emissions.

The fluorescent decay curves in $CaMoO_4$:0.5% Sm^{3+}, x% Eu^{3+} (x = 0, 1, 2, and 20) are studied for understanding the dynamical processes in energy transfer. The decay curves $I_{Sm}(t)$ for the $^4G_{5/2}$ level of Sm^{3+} are measured at 77 K by monitoring $^4G_{5/2} \rightarrow {}^6H_{9/2}$ emission at 650.5 nm as the $^4G_{5/2}$ level is excited by pulsed laser at 563.32 nm, as shown in Fig. 4. The lifetimes of Sm^{3+} $^4G_{5/2}$ level are obtained using the following expression and listed in Table 1:

$$\tau_{Sm} = \frac{1}{I_0}\int_0^\infty I_{Sm}(t)dt \qquad (1)$$

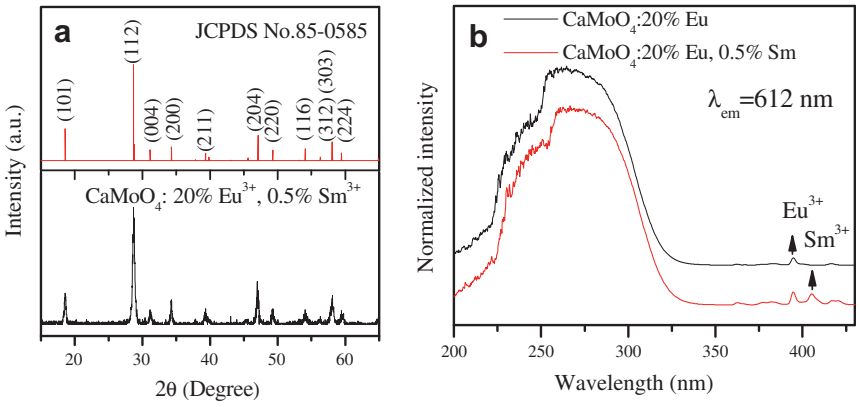

Fig. 1. (a) X-ray diffraction pattern of $CaMoO_4$:20% Eu^{3+}, 0.5% Sm^{3+}; (b) excitation spectra monitoring the $^5D_0$–$^7F_2$ emission at 612 nm of Eu^{3+} in $CaMoO_4$:20% Eu^{3+} and $CaMoO_4$:20% Eu^{3+}, 0.5% Sm^{3+}.

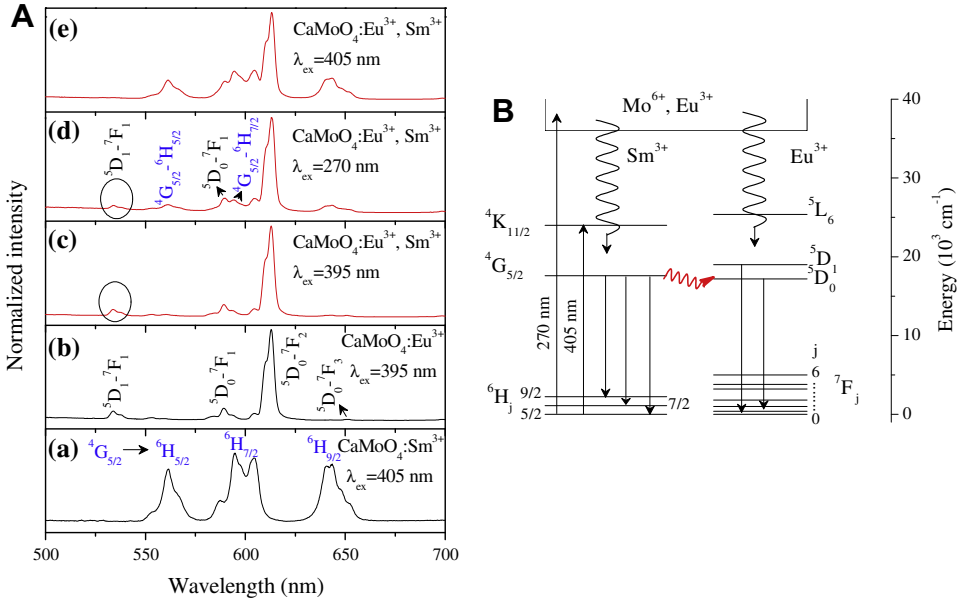

Fig. 3. (A) Emission spectra of (a) $CaMoO_4:Sm^{3+}$ (λ_{ex} = 405 nm), (b) $CaMoO_4:Eu^{3+}$ (λ_{ex} = 395 nm) and (c–d) $CaMoO_4:Eu^{3+}$, Sm^{3+} (λ_{ex} = 395 nm, 270 nm and 405 nm, respectively); (B) scheme of energy transfer pathway in $CaMoO_4:Eu^{3+}$, Sm^{3+}.

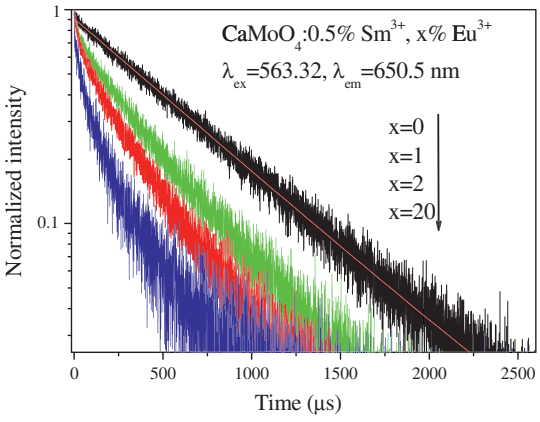

Fig. 4. Decay curves of fluorescence at 650.5 nm corresponding to $^4G_{5/2} \rightarrow {}^6H_{9/2}$ transition of Sm^{3+} in $CaMoO_4$:0.5% Sm^{3+}, *x*% Eu^{3+} (*x* = 0, 1, 2, and 20) at 77 K.

Table 1
Lifetimes of the $^4G_{5/2}$ level of Sm^{3+} in $CaMoO_4$:0.5% Sm^{3+}, *x*% Eu^{3+} (*x* = 0, 0.2, 0.5, 1, 2, 20, and 22) (λ_{ex} = 563.32 nm, λ_{em} = 650.5 nm).

Sample	$CaMoO_4$:0.5 % Sm^{3+}, *x* % Eu^{3+}						
x	0	0.2	0.5	1	2	20	22
τ (μs)	595	591	572	309	229	138	133

where I_0 is the fluorescence intensity at the time $t = 0$. As can be seen in Table 1, the lifetimes reduce with increasing Eu^{3+} content *x*, reflecting the effect of energy transfer from $^4G_{5/2}$ level of Sm^{3+} to Eu^{3+}. The decay curve is exponential for Sm^{3+} singly doped sample, i.e. $x = 0$, but non-exponential for Sm^{3+} and Eu^{3+} doubly doped sample. For the codoped samples, the non-exponential decay is resulted from the inhomogeneous energy transfer rate [17].

After Sm^{3+} is excited into its $^4G_{5/2}$ state, the energy transfer from donor Sm^{3+} $^4G_{5/2}$ to acceptor Eu^{3+} $^5D_0$ occurs. The depopulation of Sm^{3+} can be described by,

$$n_{Sm}(t) = e^{-t/\tau_{Sm}}\phi(t) \quad (2)$$

with

$$\phi(t) = \int_0^\infty f(w)e^{-wt}dw \quad (3)$$

where $n(t)_{Sm}$ is the population of $^4G_{5/2}$ of Sm^{3+} at time *t*. $f(w)$ is the distribution function of energy transfer rate *w*; τ_{Sm} is the intrinsic lifetime of the $^4G_{5/2}$ level, which is determined to be 595 μs from the exponential decay curve in $CaMoO_4$:0.5% Sm^{3+}. $\phi(t)$ denotes the loss of excited Sm^{3+} ions due to energy transfer to Eu^{3+}. If the energy transfer rate between a donor and an acceptor is proportional to an inverse power of the distance *r*, the rate may be written as α/r^m, where α is the coefficient for the energy transfer, $m = 6$, 8, 10 for dipole–dipole, dipole–quadrupole, and quadrupole–quadrupole interactions, respectively. According to Inokuti and Hirayama formula [18], one has,

$$\phi(t) = \exp\left[-\frac{4}{3}\pi\Gamma\left(1-\frac{3}{m}\right)n_a\alpha^{3/m}t^{3/m}\right] \quad (4)$$

where $\Gamma(x)$ denotes the gamma function, n_a is the number of acceptors per unit volume. From Eqs. (2) and (4), $\ln\{-\ln[n_{Sm}(t)]-t/\tau_{Sm}\}$ acts as a linear function of $\ln(t)$ with a slop of $3/m$. To understand the interaction mechanism between Sm^{3+} and Eu^{3+}, the Sm^{3+} fluorescence decay pattern is chosen as $n_{Sm}(t)$. Fig. 5a shows the ln–ln plot of $-\ln(n_{Sm}(t))-t/\tau_{Sm}$ vs time *t* for the sample $CaMoO_4$:0.5% Sm^{3+}, 2% Eu^{3+}. It is demonstrated that the slope is more close to 3/6 (red[1] line) rather than 3/8 (green line) and/or 3/10, indicating an electric dipole–dipole energy transfer with $m = 6$. Fig. 5b shows that the plot of $n_{Sm}(t)\exp(t/\tau_{Sm})$ vs $t^{1/2}$ is a linear pattern with a slop of $4\pi^{3/2}n_a\alpha^{1/2}/3$, as described by Eq. (4). From the slop of the linear pattern, $\alpha = 8.5 \times 10^{-40}$ s^{-1} cm^6 is obtained, where n_a, the number of acceptor Eu^{3+} ions per unit volume is given by 2% N_{Ca} with $N_{Ca} = 1.284 \times 10^{22}$ cm^{-3} being the number of Ca sites per unit volume in $CaMoO_4$ matrix. In $CaMoO_4$, the nearest Ca–Ca distance r_0 is 0.3896 nm and a Ca^{2+} ion has four Ca^{2+} ions as nearest neighbors. In the present sample with Eu^{3+} fractional concentration of 0.02, the initial energy transfer rate due to Sm^{3+} to the nearest Eu^{3+} can be estimated by $0.02 \times 4\alpha/r_0^6$, which yields the rate to be

[1] For interpretation of color in Fig. 5a, the reader is referred to the web version of this article.

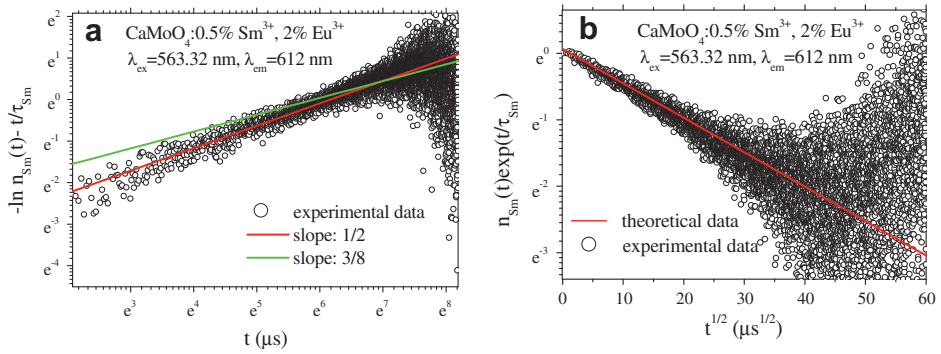

Fig. 5. (a) ln–ln plot of $-\ln(n_{Sm}(t))-t/\tau_{Sm}$ vs time t in $CaMoO_4$:0.5% Sm^{3+}, 2% Eu^{3+} at 77 K; (b) plot of $n_{Sm}(t)\exp(t/\tau_{Sm})$ vs $t^{1/2}$ in $CaMoO_4$:0.5% Sm^{3+}, 2% Eu^{3+} at 77 K.

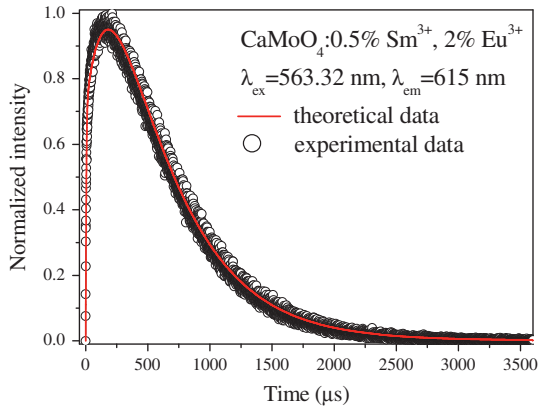

Fig. 6. Rise and decay pattern of fluorescence at 615 nm corresponding to Eu^{3+} $^5D_0 \rightarrow {}^7F_2$ transition in $CaMoO_4$:0.5%Sm^{3+}, 2%Eu^{3+} as Sm^{3+} $^4G_{5/2}$ level is only excited by pulsed laser at 563.32 nm at 77 K.

$1.9 \times 10^4\ s^{-1}$. Meanwhile, the initial energy transfer rate obtained by subtracting the radiative rate from the initial fluorescence decay rate in the sample with 0.5% Sm^{3+} and 2% Eu^{3+} is $2.0 \times 10^4\ s^{-1}$, which is slightly larger than the calculated value, indicating that the nearest Sm^{3+}–Eu^{3+} pairs govern the initial energy transfer.

Owing to $Sm^{3+} \rightarrow Eu^{3+}$energy transfer, after pulsed excitation of Sm^{3+} $^4G_{5/2}$, the populations of Eu^{3+} $^5D_0$ satisfies the following rate equation:

$$dn_{Eu}(t)/dt = -n_{Eu}(t)/\tau_{Eu} + wn_{Sm}(t) \quad (5)$$

where n_{Eu} is the population of the $^5D_0$ of Eu^{3+}, τ_{Eu} is the intrinsic lifetime of $^5D_0$. Using Eqs. (2), (3), and (5), we obtain

$$n_{Eu}(t) = e^{-t/\tau_{Eu}} \int_0^{\infty} \times \frac{wf(w)}{w + 1/\tau_{Sm} - 1/\tau_{Eu}} \left(1 - e^{-(w+1/\tau_{Sm}-1/\tau_{Eu})t}\right) dw \quad (6)$$

In the case of electric-dipole–dipole interaction with $m = 6$, the transfer rate distribution function $f(w)$ is written as [19]

$$f(w) = \frac{2\pi n_a \alpha^{1/2}}{3w^{3/2}} \exp\left(-\frac{4\pi^3 n_a^2 \alpha}{9w}\right) \quad (7)$$

Using Eq. (6), a numerical calculation for simulating the rise and decay pattern of fluorescence from $^5D_0$ of Eu^{3+} in $CaMoO_4$:0.5% Sm^{3+}, 2% Eu^{3+} is perfectly performed, as shown in Fig. 6. In the calculation, $\tau_{Eu} = 470$ μs is applied, which is obtained from the exponential decay pattern of $^5D_0 \rightarrow {}^7F_2$ fluorescence in 2% Eu^{3+} singly doped $CaMoO_4$. As one can see, the decay curve of Eu^{3+} $^5D_0$ level is composed of a rising edge starting from zero and a falling decay. It indicates that the populations of $^5D_0$ level of Eu^{3+} are completely fed by Sm^{3+} $^4G_{5/2}$ through energy transfer.

4. Conclusions

In $CaMoO_4$:Sm^{3+}, Eu^{3+}, when the $^4K_{11/2}$ of Sm^{3+} is excited, the excited $^4K_{11/2}$ relaxes down to the $^4G_{5/2}$ of Sm^{3+} itself rather than transfers to Eu^{3+}. The $Sm^{3+} \rightarrow Eu^{3+}$ energy transfer performs through the pathway from Sm^{3+} $^4G_{5/2}$ state to Eu^{3+} $^5D_0$ state rather than Eu^{3+} $^5D_1$ state. The electronic dipole–dipole interaction between Sm^{3+} and Eu^{3+} governs the transfer dynamical processes with the coefficient for the energy transfer of $8.5 \times 10^{-40}\ s^{-1}\ cm^6$. As the $^4K_{11/2}$ of Sm^{3+} is only excited, the fluorescent rise and decay pattern of Eu^{3+} $^5D_0$ state is well simulated based on $Sm^{3+} \rightarrow Eu^{3+}$ dipole–dipole energy transfer model.

Acknowledgments

This work is financially supported by the National Nature Science Foundation of China (10834006, 10774141, 10904141, 10904140), the MOST of China (2006CB601104), the Scientific project of Jilin province (20090134, 20090524) and CAS Innovation Program, the Youth Foundation of Chongqing University of Technology.

References

[1] S. Nakamura, T. Mukai, M. Senoh, J. Appl. Phys. 76 (1994) 8189.
[2] Z.G. Wei, L.D. Sun, C.S. Liao, C.H. Yan, S.H. Huang, Appl. Phys. Lett. 80 (2002) 1447.
[3] D.K. Williams, B. Bihari, B.M. Tissue, J.M. McHale, J. Phys. Chem. B 102 (1998) 916.
[4] M. Yu, J. Lin, J. Fang, Chem. Mater. 17 (2005) 1783.
[5] Z.H. Li, J.H. Zeng, Y.D. Li, Small 3 (2007) 438.
[6] N. Hirosaki, R.J. Xie, K. Kimoto, T. Sekiguchi, Y. Yamamoto, T. Suehiro, M. Mitomo, Appl. Phys. Lett. 86 (2005) 211905.
[7] J.S. Kim, P.E. Jeon, Y.H. Park, J.C. Choi, H.L. Park, G.C. Kim, T.W. Kim, Appl. Phys. Lett. 85 (2004) 3696.
[8] Y.S. Hu, W.D. Zhuang, H.Q. Ye, D.H. Wang, S.S. Zhang, X.W. Huang, J. Alloys Compd. 390 (2005) 226.
[9] J G Wang, X.P. Jing, C.H. Yan, J.H. Lin, J. Electrochem. Soc. 152 (2005) G186.
[10] J. Liu, H.Z. Lian, C.S. Shi, Opt. Mater. 29 (2007) 1591.
[11] S.X. Yan, J.H. Zhang, X. Zhang, S.Z. Lu, X.G. Ren, Z.G. Nie, X.J. Wang, J. Phys. Chem. C 111 (2007) 13256.
[12] C.L. Zhao, Y.S. Hu, W.D. Zhuang, X.W. Huang, T. He, J. Rare Earths 27 (2009) 758.
[13] Y. Jin, J.H. Zhang, S.Z. Lu, H.F. Zhao, X. Zhang, X.J. Wang, J. Phys. Chem. C 112 (2008) 5860.
[14] W.W. Holloway JR., M. Kestigian, J. Opt. Soc. Am. 56 (1966) 1171.
[15] Z. Wang, H. Liang, M. Gong, Q. Su, Electrochem. Solid-State Lett. 8 (2005) H33.
[16] X. Wang, Y. Xian, G. Wang, J. Shi, Q. Su, M. Gong, Opt. Mater. 30 (2007) 521.
[17] J. Hegarty, D.L. Huber, W.M. Yen, Phys. Rev. B 23 (1981) 6271.
[18] M. Inokuti, F. Hirayama, J. Chem. Phys. 43 (1965) 1978.
[19] S. Huang, L. Lou, J. Lumin. 45 (1990) 377.